

*Simulation Tool for Variably Saturated Flow
with Comprehensive Geochemical Reactions in
Two- and Three-Dimensional Domains*

L. Wissmeier*, D.A. Barry

Ecole Polytechnique Fédérale de Lausanne (EPFL)

Laboratoire de Technologie Ecologique

Station 2, CH-1015 Lausanne, Switzerland

Resubmitted on 17 August 2010 to Environmental Modelling & Software

* Author to whom all correspondence should be addressed. Telephone: +41 21 693 5727, facsimile: +41 21 693 8035

E-mail addresses: laurin.wissmeier@epfl.ch (L. Wissmeier), andrew.barry@epfl.ch (D.A. Barry)

1 **Abstract**

2 We present a software tool for simulations of flow and multi-component solute transport in
3 two and three-dimensional domains in combination with comprehensive intra-phase and
4 inter-phase geochemistry. The software uses IPhreeqc as a reaction engine to the multi-
5 purpose, multidimensional finite element solver COMSOL Multiphysics® for flow and
6 transport simulations. Here we used COMSOL to solve Richards' equation for aqueous phase
7 flow in variably saturated porous media. The coupling procedure presented is in principle
8 applicable to any simulation of aqueous phase flow and solute transport in COMSOL. The
9 coupling with IPhreeqc gives major advantages over COMSOL's built-in reaction capabilities,
10 i.e., the soil solution is speciated from its element composition according to thermodynamic
11 mass action equations with ion activity corrections. State-of-the-art adsorption models such
12 as surface complexation with diffuse double layer calculations are accessible. In addition,
13 IPhreeqc provides a framework to integrate user-defined kinetic reactions with possible
14 dependencies on solution speciation (i.e., pH, saturation indices, and ion activities), allowing
15 for modelling of microbially mediated reactions. Extensive compilations of geochemical
16 reactions and their parameterization are accessible through associated databases.

17 **Keywords**

18 Geochemistry, Reaction, PHREEQC, IPhreeqc, Richards' Equation, Unsaturated Flow,
19 COMSOL, Solute Transport

20 **Research highlights**

- 21 • Coupling of COMSOL and PHREEQC facilitates simulation of variably saturated flow
22 with comprehensive geochemical reactions.
- 23 • The use of finite elements allows for the simulation of flow and solute transport in
24 complex 2 and 3D domains.
- 25 • Geochemical reactions are coupled via sequential non-iterative operator splitting.
- 26 • The software tool provides novel capabilities for investigations of contaminant
27 behaviour in variably saturated porous media and agricultural management.

28 **Software requirements**

29 COMSOL Multiphysics® including Earth Science Module (tested version: 3.5a; due to a
30 memory leak in versions 4.0 and 4.0a, these are not suitable for the presented coupling)
31 Price for single user academic license including Earth Science Module ca. 2000 €

32 Matlab® (tested versions: 7.9, 7.10)

33 Price for single user academic license including Parallel Computing Toolbox ca. 650 €

34 IPhreeqc (COM-version, available free of charge at

35 http://wwwbrr.cr.usgs.gov/projects/GWC_coupled/phreeqc/)

36 The coupling files together with animations of the presented simulations are available at

37 <http://infoscience.epfl.ch/record/143469> (link: download fulltext)

38 **1 Introduction**

39 Computer simulations of water availability and quality play an important role in state-of-
40 the-art water resources management and agriculture (Barry, 1992; Šimůnek and Bradford,
41 2008). Due to the importance of the unsaturated zone as the major life-supporting
42 ecosystem on land (Brussaard et al., 2007), there is a great demand for understanding and
43 predicting the complex interactions between highly non-linear vadose zone flow and bio-
44 geochemical reactions (Wissmeier et al., 2009). However, many of the most utilized
45 software programs focus either on physical flow and transport phenomena (e.g., MODFLOW
46 (Harbaugh et al., 2000), SUTRA (Voss and Provost, 2008), HYDRUS (Šimůnek et al., 2009)), or
47 on geochemical reactions (e.g., MINTEQ (Gustafsson, 2010), CHESS (van der Lee, 1998),
48 ORCHESTRA (Meeussen, 2003)). Saturated flow codes have been coupled with geochemical
49 reaction packages to produce combined water flow, multispecies transport and complex
50 geochemical reactions (e.g., PHT3D (Prommer et al., 1999), DART (Freedman and Ibaraki,
51 2002), PHAST (Parkhurst et al., 2004), PHWAT (Mao et al., 2006). In recent years, simulation
52 tools for unsaturated porous media flow with detailed geochemistry have emerged (HP1
53 (Šimůnek et al., 2009), RICH-PHREEQ (Wissmeier and Barry, 2010)). Although powerful tools,
54 the applicability of the aforementioned unsaturated flow/transport/reaction models is
55 restricted to systems with one-dimensional movement of water and solutes.

56 The coupling of COMSOL (COMSOL Multiphysics®, 2010) and IPhreeqc (Charlton and
57 Parkhurst, 2010) presented here extends the capabilities of these models by combining
58 unsaturated porous media flow in two and three dimensions with comprehensive
59 geochemical reactions. IPhreeqc is a version of PHREEQC (Parkhurst and Appelo, 1999) that
60 is specifically designed for coupling to multicomponent transport simulators. While it retains
61 all of PHREEQC's reaction capabilities, IPhreeqc provides additional methods for data
62 manipulation and communication to the host application. The coupled model's main
63 features are listed below.

64 Unsaturated Flow:

- 65 • Constitutive relations according to van Genuchten (1980), Brooks and Corey (1964) or
- 66 user-defined
- 67 • Anisotropic unsaturated conductivity

- 68 • Specific storage according to fluid compressibility or user-defined storability function
- 69 • Fluid density, viscosity and liquid source term through user-defined expressions with
- 70 possible dependencies on COMSOL variables

71 Multispecies Solute Transport:

- 72 • Dispersivity in directions parallel and orthogonal to flow
- 73 • Tortuosity according to Millington and Quirk (1961) or user-defined
- 74 • Species independent coefficient of molecular diffusion and dispersivities
- 75 • Liquid source concentrations and solute sources through user-defined expressions with
- 76 possible dependencies on COMSOL variables

77 Geochemical Reactions:

- 78 • Equilibrium solution speciation and redox reactions
- 79 • Equilibrium mineral dissolution/precipitation
- 80 • Ion exchange on permanently charged adsorption sites
- 81 • Surface adsorption according to the diffuse double layer model (Dzombak and Morel,
- 82 1990) or the CD_MUSIC model (Hiemstra et al., 1989) with or without explicit calculation
- 83 of the diffuse double layer composition
- 84 • Kinetic reactions according to user-defined rate equations, with possible dependencies
- 85 on solution speciation, temperature or moisture content
- 86 • Gas phase exchange
- 87 • Solid solutions

88 A considerable advantage of the coupling results from the flexibility of COMSOL to define
89 any input parameter as a function of internal variables. For example, root water uptake,
90 entered as a negative liquid sources term, can be defined by a function of space coordinates
91 and liquid phase pressure head. In addition, IPhreeqc's capabilities to integrate user-defined
92 rate expressions allows for the simulation of complex time-dependent geochemical
93 reactions with explicit dependencies on solution speciation (e.g., ion activities, pH, mineral
94 saturation). With these capabilities, the presented model is significantly more
95 comprehensive than existing codes in the field of unsaturated reactive transport modelling,
96 such as MIN3P (Mayer et al., 2002) and RETRASO (Saaltink et al., 2004). The model setup is

97 greatly facilitated by graphical user interfaces for flow and transport (COMSOL) and
98 reactions (PHREEQC).

99 This paper is organized as follows. Section 2 briefly describes the underlying theory of
100 component-based phase flow, section 3 illustrates the coupling procedure, and sections 4
101 and 5 provide application examples for kinetic pesticide degradation and fertigation via a
102 subsoil drip irrigation system (files for these cases are available for download).

103 **2 Theory**

104 In the presented scheme, the classical advection diffusion/dispersion equation was used for
105 multi-component solute transport (Bear, 1972, 2007; Bear and Bachmat, 1998),

$$\frac{\partial \theta c_i}{\partial t} = -\nabla \cdot (\mathbf{q} c_i) + \nabla \cdot (\theta \bar{\mathbf{D}} \nabla c_i), \quad (1)$$

106 where θ is the relative liquid phase saturation ($\text{m}^3 \text{m}^{-3}$), c_i (kg m^{-3}) is the concentration of
107 solution species i , \mathbf{q} (m s^{-1}) is the Darcy flux and $\bar{\mathbf{D}}$ ($\text{m}^2 \text{s}^{-1}$) is the hydrodynamic dispersion
108 tensor.

109 Recognizing that the liquid phase is composed of solution species according to

$$\theta = \frac{\sum_i n_i m_i}{\rho}, \quad (2)$$

110 where n_i (mol m^{-3}) is the moles of solution species i in a control volume with a molar weight
111 m_i (kg mol^{-1}), the application of Eq. (1) to all solution species in the liquid phase effectively
112 yields phase mass balance according to

$$\frac{\partial \rho \theta}{\partial t} = -\nabla \cdot \rho \theta \mathbf{v}, \quad (3)$$

113 where \mathbf{v} is the barycentric mass flow velocity of the liquid phase (Corey and Auvermann,
114 2003). This implies that the net mass flux induced by diffusion/dispersion (Letey et al., 1969)
115 can be neglected, which is a common assumption (Jacques and Šimůnek, 2010; Miller et al.,
116 1998; Šimůnek et al., 2006; Šimůnek et al., 2009).

117 In the presented scheme, the Darcy flux $\mathbf{q} = \mathbf{v}\theta$ (m s^{-1}) is computed from Richards'
118 equation according to

$$\mathbf{q} = \frac{\bar{\bar{\mathbf{K}}}}{\rho g} (\nabla p + \rho g \nabla z), \quad (4)$$

119 (e.g., Bear, 1972, 2007), where $\bar{\bar{\mathbf{K}}}$ is the unsaturated hydraulic conductivity tensor (m s^{-1}), p
120 is the fluid pressure ($\text{kg m}^{-1} \text{s}^{-2}$) and g is the magnitude of gravitational acceleration (m s^{-2}).

121 The other major part of the model concerns geochemical reactions (including biological
122 reactions modelled using a geochemical approach). Thorough descriptions of the models for
123 this part are available in textbooks (Appelo and Postma, 2005; Langmuir, 1997) and the
124 PHREEQC manual (Parkhurst and Appelo, 1999).

125 **3 Coupling procedure**

126 In the discretized time domain of the numerical model, the three simultaneous and
127 dependent processes *flow*, *solute transport* and *reaction* are separated using a non-iterative
128 sequential split-operator approach where Δt is the length of the coupling time step. The
129 coupling time step is further reduced within the iterative schemes for unsaturated flow,
130 solute transport and geochemical speciation as required by the respective algorithms. As
131 result of the decoupling, concentrations are assumed independent of reactions in solute
132 transport computations. As well, the liquid phase saturation and density are similarly
133 assumed independent of concentrations and reactions during flow calculations. During the
134 geochemical reaction step (performed within IPhreeqc), the solution composition is
135 assumed independent of both flow and transport. The influence of reaction kinetics, grid
136 size and splitting time step on the introduced splitting error in unsaturated flow situations
137 was investigated by Jacques et al. (2006). General discussions on operator splitting are
138 provided by Yeh and Tripathi (1989), Valocchi and Malmstead (1992) and Barry et al. (2000;
139 1996; 1997), among others.

140 **Fig. 1. Program flow and structure.**

141 Fig. 1 illustrates the program structure for the coupling of COMSOL and IPhreeqc using
142 Matlab (Matlab®, 2010) as the controlling application and interface for the COMSOL and
143 IPhreeqc modules (grey shaded, dashed boxes). The code is organized in three major m-files

144 (black textboxes in Fig. 1). At the beginning of the simulation, the controlling script
145 *coupling_COMSOL_PHREEQC.m* runs subscripts to configure the simulation domain with
146 flow and transport properties, initializes COMSOL and IPhreeqc computations and specifies
147 boundary conditions. Geochemical properties such as pH and redox potential (pe) are
148 extremely sensitive to the total element concentrations. Minimal deviations of the ratio of
149 oxygen to hydrogen from the stoichiometric ratio of 1:2 in the simulation of pure water will
150 dramatically affect the pe, for example. Precise concentration values for initial and
151 boundary conditions in COMSOL are thus conveniently determined by preliminary PHREEQC
152 speciation calculations.

153 After the initialization procedure, computations enter the iteration loop of the split
154 operator, where COMSOL and IPhreeqc procedures alternate for the calculation of flow,
155 transport and reactions. Data from the output of one procedure is passed back to the
156 Matlab workspace and reformatted for the following procedure using the functions
157 *phreeqc2comsol* and *comsol2phreeqc*. For the computation of aqueous phase flow in
158 COMSOL, fluid pressures are calculated from the output of the preceding reaction step
159 (mass of solution in control volume, solution density, pressure-saturation relation). Darcy
160 flux velocities from flow calculations together with master species concentrations from the
161 reaction step are input into the COMSOL solute transport routine (Eq. (1)). The use of
162 master species instead of solution species considerably reduces the degrees of freedom in
163 transport calculations and therefore the numerical burden (Steeffel and MacQuarrie, 1996).
164 However, it impedes the simulation of species-dependent diffusion. The *comsol2phreeqc*-
165 function retrieves the results from COMSOL as a vector of all degrees of freedom (fluid
166 pressure and element concentrations) at all nodes in the domain. The vector is reformatted
167 as a numeric Matlab array. Master species concentrations from transport calculations are
168 multiplied by moisture contents from flow calculations. This yields the aqueous phase
169 composition at each node in terms of moles of master species per control volume. In the
170 IPhreeqc reaction step, each node in the simulation domain is represented by a single batch
171 reactor that contains physical amounts (moles) of solution elements, minerals, gases and
172 adsorption sites. Since only the liquid phase composition is altered through flow and
173 transport, *comsol2phreeqc* only updates the solution composition using IPhreeqc's method
174 *SOLUTION_MODIFY*. From the ensemble of elements, the aqueous solution is speciated, and

175 mineral reactions, surface adsorption/desorption reaction and kinetic reactions are
176 computed. After the IPhreeqc reaction procedure, flow and transport calculations in
177 COMSOL are reinitialized with the updated values of moisture content and master species
178 concentrations using the *phreeqc2comsol*-function. Results, which are passed back from
179 IPhreeqc to the Matlab workspace as a cell array, are reshaped as a vector with the same
180 structure of the COMSOL solution vector. COMSOL's *assemnit*-function is used to create
181 valid initial conditions for flow and transport calculations in COMSOL.

182 **All** primary master species in the liquid phase (including elemental oxygen and hydrogen)
183 must be included in solute transport calculations in order to represent flow by the transport
184 of liquid phase components. This approach has been applied in previous couplings of
185 geochemistry in PHREEQC with unsaturated flow and transport calculations (Jacques et al.,
186 2008; Wissmeier and Barry, 2010). Charge imbalance, present in initial and boundary
187 solutions or developing during reactions (e.g., surface adsorption without explicit calculation
188 of the diffuse layer composition) (Parkhurst, 2010), is treated as an extra solution
189 component in transport calculations. It is also included in speciation calculations in order to
190 accurately reproduce pH and pe.

191 During the conversion from units relative to an arbitrary control volume in COMSOL (e.g.,
192 $\text{m}^3 \text{m}^{-3}$ for θ) to physical quantities in IPhreeqc, the size of the batch reactors is taken as one
193 litre for convenience. Thus, solid phase properties in IPhreeqc, such as the moles of
194 adsorption sites and mineral phases have to be understood as per litre of unsaturated zone
195 volume (soil including pore space). Without further modifications, solid phase properties are
196 independent of water contents, i.e., the moles of mineral phases or exchange sites in
197 contact with the unsaturated soil solution do not change due to changes in moisture
198 contents.

199 Negative master species concentrations may result from oscillatory behaviour of COMSOL's
200 finite element scheme for solute transport in the vicinity of sharp concentration gradients.
201 The performance index, defined as the product of the grid Péclet number and the Courant
202 number, can be used as an indicator of oscillatory transport behaviour (Huyakorn and
203 Pinder, 1983; Perrochet and Berod, 1993; Šimůnek et al., 2009). Since IPhreeqc defines the
204 solution composition in terms of moles of elements, negative concentrations from the

205 COMSOL-procedure are set to zero during reaction calculations. After the reaction step,
206 negative concentrations from the previous flow/transport step in COMSOL are summed to
207 the master species concentrations that are output of IPhreeqc. The summation of negative
208 concentrations from transport simulations to the results from reaction calculations avoids
209 significant mass balance errors that would otherwise result from the repeated adjustment
210 of negative output from COMSOL to zero. This procedure remedies mass balance errors.
211 Nevertheless, it is recommended to avoid oscillations in solute transport through
212 appropriate domain discretisation (Donea and Huerta, 2004; Perrochet and Berod, 1993).

213 For accurate transport of pH in unbuffered solutions, the relative tolerance of the solute
214 transport scheme in COMSOL is set to 10^{-10} . In order to decrease the absolute tolerance for
215 oxygen and hydrogen, their nominal concentrations in COMSOL are reduced by their molal
216 concentrations in pure water (55.50621679636 mol_O/kg_{water} and 111.0124335927
217 mol_H/kg_{water}, respectively). Even with this high accuracy, calculations of the redox potential
218 (pe) in unbuffered solutions may not give reliable results and should be examined carefully.
219 Equilibration with atmospheric O₂ stabilizes otherwise unbuffered solutions and should
220 therefore be considered if applicable (Parkhurst and Appelo, 1999).

221 The COM-version of IPhreeqc (Charlton and Parkhurst, 2010) that is utilized in the presented
222 coupling has a number of features that greatly simplify data handling:

- 223 • Reaction calculations can be entirely controlled from within Matlab by passing
224 commands strings to the COM object.
- 225 • Changes in the reaction system due to transport of aqueous elements are considered by
226 modifying the moles of elements in solution.
- 227 • No cumbersome writing/reading of files is necessary in order to pass results from the
228 reaction module to the flow/transport module and vice versa. Data transfer via the
229 Matlab workspace is processed entirely in memory.
- 230 • The status of the entire geochemical system, including all exchangers, surfaces, kinetics
231 phases, mineral and gas phases, is automatically saved by the COM object in between
232 calls.

233 As result of persistence of the geochemical properties in the COM object, the coupling
234 procedure only needs to manage solution elements. This not only decreases programming

235 effort and increases coupling efficiency but also eliminates the need for user-defined
 236 definitions of all possible exchange and surface species, as is found in earlier couplings
 237 involving PHREEQC (Prommer et al., 2003).

238 4 Verification example: Pesticide degradation

239 This application example reproduces the simulation of kinetic pesticide degradation in
 240 COMSOL's model library (COMSOL Multiphysics®, 2008b) using IPhreeqc instead of
 241 COMSOL's Reaction Engineer Lab® to simulate the reaction chain. According to
 242 COMSOL Multiphysics® (2008b), the simulation is inspired by but does not exactly duplicate
 243 the application example no. 7 of the software packages SWMS-2D (Šimůnek et al., 1994) and
 244 HYDRUS-2D (Šimůnek et al., 1999). Because of the identical treatment of unsaturated flow
 245 and solute transport, the application example can be regarded as a verification of the
 246 coupling procedure.

247 **Fig. 2. Simulation domain with finite element mesh for pesticide simulation. The source zone is indicated by the thick**
 248 **line at $y = 0$.**

249 The radially symmetric simulation domain with 4401 nodes and 26406 degrees of freedom is
 250 displayed in Fig. 2. The pesticide *Aldicarb* enters the dry soil via constant flux infiltration at
 251 the top boundary in the region $y = 0$ m, $0 \text{ m} \leq r \leq 0.2$ m. The soil is divided into two
 252 subdomains with different hydraulic properties, i.e., higher conductivity and lower saturated
 253 water content below $y = -0.4$ m. The initial hydraulic head h (m) of the simulation domain is
 254 given by the expression

$$h(y) = \begin{cases} -(y + 1.2 \text{ m}), & y < -0.4 \text{ m}, \\ -(1.2y + 1.6 \text{ m}), & y \geq -0.4 \text{ m}. \end{cases} \quad (5)$$

255 Transformations between Aldicarb and its breakdown products are governed by first-order
 256 rates according to Eqs. (6-11), where n_i denotes moles of the chemical in the control
 257 volume (mol m^{-3}), $k_1 - k_5$ are reaction constants (s^{-1}), c'_i denote total molal concentrations
 258 ($\text{mol kg}_{\text{water}}^{-1}$) and w stands for the kilograms of water in the control volume (kg m^{-3}).

Aldicarb (a):

$$\frac{\partial n_a}{\partial t} = -(k_1 c'_a + k_2 c'_a)w; \quad (6)$$

$$\text{Aldicarb Oxime (ao):} \quad \frac{\partial n_{ao}}{\partial t} = k_1 c'_a w; \quad (7)$$

$$\text{Aldicarb Sulfoxide (asx):} \quad \frac{\partial n_{asx}}{\partial t} = (k_2 c'_a - k_3 c'_{asx} - k_4 c'_{asx}) w; \quad (8)$$

$$\text{Aldicarb Sulfoxide Oxime (asxo):} \quad \frac{\partial n_{asxo}}{\partial t} = k_3 c'_{asx} w; \quad (9)$$

$$\text{Aldicarb Sulfone (asn):} \quad \frac{\partial n_{asn}}{\partial t} = -(k_4 c'_{asn} + k_5 c'_{asn}) w; \quad (10)$$

$$\text{Aldicarb Sulfone Oxime (asno):} \quad \frac{\partial n_{asno}}{\partial t} = k_5 c'_{asn} w. \quad (11)$$

259 The reaction chain together with first-order rate constants is displayed schematically in Fig.
260 3.

261 **Fig. 3. Aldicarb reaction chain.**

262 To be consistent with the COMSOL example, it is necessary to prevent unwanted
263 geochemical transformations. Therefore, Aldicarb and its daughter products were
264 introduced into IPhreeqc as separate uncharged solution master species with no reactions
265 apart from the transformations listed in Fig. 3. Further details of the breakdown process and
266 the COMSOL solution are available in the COMSOL model library documentation
267 (COMSOL Multiphysics®, 2008a). The coupling time step Δt was set to 0.1 d.

268 **Fig. 4. Comparison of concentrations from the coupling procedure and COMSOL alone eight d after beginning of**
269 **infiltration.**

270 In order to verify the coupling procedure, moisture content and concentrations were
271 compared along the centre line ($r = 0$) with results from COMSOL alone (Fig. 4). Moisture
272 contents from the coupled simulation (COMSOL+IPhreeqc) and the global implicit method in
273 COMSOL (COMSOL) are visually indistinguishable. Small differences in chemical
274 concentrations can be fully attributed to the splitting error, whose magnitude decreases
275 linearly with Δt . If negative concentrations from the previous transport step are not
276 summed to the concentrations after transport, as described in section 3, an obvious mass
277 balance error with overestimation of all pesticide species is produced. Thus, the results
278 prove the accuracy of the coupling procedure and particularly the successful suppression of
279 significant mass balance errors that would result from the uncompensated adjustment of
280 concentrations to positive values during reaction calculations.

281 **5 Application example: Drip irrigation and fertigation**

282 This example, reported by Hanson et al. (2006), simulates the fertigation of a tomato
283 plantation using a subsoil micro-irrigation system with periodic input of water and fertilizer
284 solution. The simulation of flow and transport was reproduced in COMSOL using the same
285 domain properties and parameters as in Hanson et al. (2006), who applied HYDRUS-2D
286 (Šimůnek et al., 1999). In contrast to Hanson et al. (2006), however, we implemented a
287 detailed description of geochemical through the coupling to IPhreeqc. This included solution
288 speciation with ion activity correction, kinetic redox transformations and cation exchange.
289 In agreement with Hanson et al. (2006), root water uptake was simulated using the spatial
290 root distribution model of Vrugt et al. (2001) in combination with the water stress response
291 function of Feddes et al. (1978). The model was implemented through the Matlab function
292 *root_uptake.m*, which is called from COMSOL at runtime (details on root water uptake are
293 given by Šimůnek and Hopmans, 2009; Šimůnek et al., 1999).

294 **Fig. 5. Simulation domain with finite element mesh for drip irrigation simulation.**

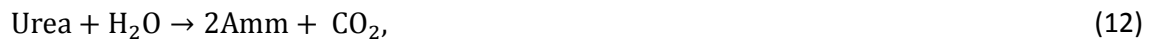
295 The simulation domain with 2665 nodes and 23985 degrees of freedom is displayed in Fig. 5.
296 It represents a 2D slice of the soil system with axial symmetry along the left boundary.
297 Solutes and irrigation water enter the soil through the small half circle at $x = 0$ m, $y = -0.2$ m
298 that represents the irrigation pipe with a diameter of 0.02 m. Irrigation imposes a constant
299 flux for 1.15 d intermittent with no flow periods of 2.35 d. The fertilizer enters the domain
300 for 0.575 d via a constant concentration boundary beginning 0.2875 d after start of
301 irrigation periods. Details of the flow and solute transport properties are given by Hanson et
302 al. (2006) and Gärdenäs et al. (2005) (simulation *SUBTAPE*, fertigation scenario *M50*).

303 Master species concentrations in the inflowing fertilizer solution were calculated by reacting
304 0.1449 mol KH_2PO_4 , 0.0362 mol NH_4NO_3 [AmmHNO₃] and 0.0725 mol $(\text{NH}_2)_2\text{CO}$ [Urea] with
305 1 kg of pure water. In order to prevent instantaneous hydrolysis and nitrification, urea
306 (Urea) and ammonia (Amm) were defined as separate solution master species in IPhreeqc.
307 In addition, the fertilizer solution and the fertilizer-free irrigation water were equilibrated
308 with atmospheric CO_2 ($10^{-3.5}$ atm) and O_2 ($10^{-0.7}$ atm). The initial soil solution was assumed in
309 equilibrium with atmospheric O_2 ($10^{-0.7}$ atm) and with CO_2 from root respiration at a partial
310 pressure $10^{-1.5}$ atm. The latter value was chosen in agreement with the expected high actual
311 evaporation (~ 1200 mm yr^{-1}) for an irrigated tomato plantation in California, USA (Hanson et

312 al., 2006) according to Brook et al. (1983). Properties of inflowing and initial solutions are
 313 summarized in Table 1.

314 **Table 1**
 315 **Geochemical solution properties. Master species concentrations in mol kg_{water}⁻¹, truncated to 2 digits.**

316 Equilibrium solution speciation was defined as given in the thermodynamic database
 317 *phreeqc.dat*, which is distributed with IPhreeqc. In order to suppress denitrification as in
 318 Hanson et al. (2006), the equilibrium constant for the reaction $2\text{NO}_3^- + 12\text{H}^+ + 10\text{e}^- \rightleftharpoons \text{N}_2 +$
 319 $6\text{H}_2\text{O}$ was set to 10^{-1000} . Kinetic hydrolysis of urea was simulated according to the reaction



320 with the first-order rate expression r_{hyd} (mol s⁻¹ m⁻³) (Hanson et al., 2006),

$$r_{\text{hyd}} = k_{\text{hyd}} c'_{\text{Urea}} w, \quad (13)$$

321 where k_{hyd} is the reaction constant taken as -0.35 d⁻¹ and c'_{Urea} is the molal urea
 322 concentration. For the kinetic nitrification of ammonium to nitrate, we used the reaction
 323 formula



324 with the rate,

$$r_{\text{nit}} = k_{\text{nit}} c'_{\text{Amm}} w \frac{c'_{\text{O}(0)}}{c'^0_{\text{O}(0)}}. \quad (15)$$

325 The reaction constant k_{nit} was set to -0.2 d⁻¹. In Eq. (15), c'_{Amm} and $c'_{\text{O}(0)}$ are the molal
 326 concentrations of ammonium and zero-valent oxygen, respectively, and $c'^0_{\text{O}(0)}$ is the
 327 concentration of zero-valent oxygen in the initial solution (5.11×10^{-4} mol kg_{water}⁻¹). The last
 328 term in Eq. (15) was introduced as an additional factor to the rate expression of Hanson et
 329 al. (2006). Its purpose is to simulate free oxygen as a rate-limiting redox partner for the
 330 kinetic oxidation of ammonium to nitrate.

331 In contrast to Hanson et al. (2006), who used a simple linear isotherm for ammonium
 332 adsorption, we simulated adsorption of aqueous cations on negatively charged surfaces as a
 333 cation exchange process (Appelo and Postma, 2005). Besides potassium and ammonium,

334 free protons (H^+) are included in the competition for the exchange sites in order to consider
335 the pH dependence of cation exchange and to be consistent with the conceptualization of
336 plant nutrient uptake via proton exchange (Hedrich and Schroeder, 1989). The cation
337 exchange capacity was taken as $150 \text{ meq } l_{\text{soil}}^{-1}$, which is a reasonable value for loam
338 (Yukselen and Kaya, 2006). Exchange reaction formulas and ion affinities with suggested
339 values for proton exchange were those included in the database *phreeqc.dat*. The split-
340 operator time step Δt for the alternation between transport and reactions calculations was
341 set to 0.01 d.

342 **Fig. 6. Normalized root distribution according to the Vrugt model (Vrugt et al., 2001) with parameters from Hanson et al.**
343 **(2006).**

344 Fig. 6 displays the normalized root distribution function used to describe water and solute
345 losses due to plant water uptake. As required by the Vrugt model (Vrugt et al., 2001), the
346 normalized root distribution integrates to unity over the simulation domain. Clearly visible
347 in Fig. 7 is the decrease of root density at depths $y < -0.2 \text{ m}$, which is determined by the
348 parameter z^* in Hanson et al. (2006).

349 **Fig. 7. Moisture contents at 0 and 1.15 d, i.e., the beginning and end of the first irrigation period; white contours: lines of**
350 **equal water contents.**

351 The successful re-simulation of moisture dynamics was verified by visually comparing
352 moisture contents at the beginning and end of the first irrigation period with results
353 presented in Gärdenäs et al. (2005) and Hanson et al. (2006) (To follow this comparison the
354 reader is referred to the original references). The comparison reveals small discrepancies in
355 the dry part of the domain and along the right no-flow boundary, which can be attributed to
356 different domain discretizations and tolerance settings in the numerical methods.

357 **Fig. 8. Solution master species concentrations 3.88, 4.63, 5, 7 and 28 d after beginning of fertigation cycles.**

358 Molal concentrations of all solution master species, except for oxygen, hydrogen and
359 carbon, are displayed in Fig. 8. In the model phosphorus (P) is not involved in any kinetic
360 reactions or adsorption/desorption processes (since it does not adsorb to negatively
361 charged sorption sites) and therefore can be used as a reference for conservative solute
362 transport. By comparison to phosphorus and from concentrations of $O(0)$ in Fig. 9 it is
363 evident that the kinetic transformation of ammonium to nitrate is limited by the available
364 $O(0)$. Urea is clearly affected by hydrolysis with decreasing concentrations after fertigation
365 periods and increasing concentrations of ammonia (Amm). Potassium (K) is strongly

366 retarded compared to phosphorus, with equal inflowing and initial concentrations due to
367 exchange with adsorbed protons and ammonia.

368 **Fig. 9. Moisture contents, pH and exchanger composition 3.88, 4.63, 5, 7 and 28 d after beginning of fertigation cycles.**

369 The exchanger composition, pH and molal concentrations of O(0) are presented in Fig. 9.
370 The soil's low initial pH originates from respiratory CO₂. The decreasing pH behind the solute
371 front can be attributed to (i) oxidation of ammonium and (ii) the replacement of protons
372 from the surface exchange sites by ammonia and potassium. The latter can be interpreted
373 as a proton "snow plough" (Barry et al., 1983).

374 Low pH values due to nitrification and proton exchange may result in significant dissolution
375 of soil matrix minerals (e.g., calcite), which may act as pH buffers and release cations that
376 compete for adsorption sites and thereby reduce the adsorption efficiency of fertilizer ions.
377 Kinetic or equilibrium mineral reactions can be easily included in the simulation. However,
378 this was not taken into account in the given example because of the unknown mineral
379 composition of the substrate. Kinetic oxidation of ammonium to nitrate leads to a local
380 depletion in O(0) concentrations that inhibits further nitrification according to Eq. (15). Due
381 to the absence of other cations, the initial exchanger is entirely filled with H⁺. This situation
382 is unlikely to be valid in the field, but allows for more straightforward interpretation of this
383 illustration. A more realistic exchanger initialization requires measured exchanger
384 compositions or knowledge about the trace elements in the initial soil solution. Even though
385 the exchanger has a slightly larger affinity for potassium, ammonium dominates the
386 exchanger composition in the exterior of the solute ring that forms around the irrigation
387 pipe. This is due to the elevated concentration of ammonium from urea hydrolysis and
388 retardation of potassium, which shifts the concentration ratio towards ammonium. In
389 addition, the low pH values in this region favour the formation of ammonium as opposed to
390 non-adsorbing ammonia. Potassium is mainly adsorbed close to the irrigation pipe, where
391 ammonium concentrations are low. The region at $x = 0.6$ m, $y = 0$ m remains extremely dry
392 (cf. Fig. 7). Therefore, it is effectively inert towards changes in geochemical conditions (e.g.,
393 pH, O(0) content).

394 Results of the present simulation and those of Hanson et al. (2006) show roughly similar
395 patterns for nitrate and urea. However, in our simulations nitrate concentrations at 7 and 28

396 d are considerably lower in the direct vicinity of the supply tube, where it shows the highest
397 concentrations in Hanson et al. (2006). The lower concentration in our simulations is
398 expected considering the irrigation/fertigation scheme where the fertilizer is flushed into
399 the soil with pure water following its application.

400 **6 Concluding remarks**

401 The application example in section 4 verifies the coupling of unsaturated flow and
402 multispecies solute transport in COMSOL with the geochemical modelling framework
403 IPhreeqc. Minor differences to the global implicit solution are introduced through operator
404 splitting and can be controlled by the magnitude of the splitting time step Δt . Furthermore,
405 it was shown that the constraint of positive concentrations in IPhreeqc in combination with
406 negative concentrations from COMSOL's solute transport scheme does not lead to
407 significant mass balance errors.

408 Section 5 shows the enhanced geochemical capabilities resulting from the coupling between
409 COMSOL and IPhreeqc in a complex simulation of unsaturated flow and solute transport.
410 The successful replication of the moisture content distribution from Hanson et al. (2006)
411 illustrates the capabilities of COMSOL's Earth Science Module to simulate unsaturated flow
412 processes. Further, the implementation of pressure- and root distribution-dependent root-
413 water uptake demonstrates the convenience of COMSOL to extend predefined vadose zone
414 processes through user-defined Matlab functions.

415 Due to the capabilities of COMSOL to simulate a wide variety of environmental flow
416 phenomena (e.g., two-phase flow, fracture flow, flow according to the Darcy, Brinkman or
417 incompressible Navier-Stokes equations), the presented coupling procedure can be utilized
418 as a general guide for linking flow and transport calculations in COMSOL to geochemical
419 reactions in IPhreeqc.

420 **Acknowledgments**

421 The authors wish to thank David Parkhurst and Tony Appelo for their assistance with the
422 coupling procedure and the prompt implementation of the required features into PHREEQC.

423 This research was supported by Alcoa World Alumina Australia.

424 **References**

- 425 Appelo, C.A.J., Postma, D., 2005. *Geochemistry, Groundwater and Pollution*, 2nd ed.
426 Balkema, Leiden, Netherlands, 649 pp.
- 427 Barry, D.A., 1992. Modelling contaminant transport in the subsurface: Theory and computer
428 programs, In: Ghadiri, H., Rose, C.W. (Eds.), *Modelling Chemical Transport in Soil:*
429 *Natural and Applied Contaminants*. Lewis Publishers: Boca Raton, Florida, pp. 105-
430 144.
- 431 Barry, D.A., Bajracharya, K., Crapper, M., Prommer, H., Cunningham, C.J., 2000. Comparison
432 of split-operator methods for solving coupled chemical non-equilibrium
433 reaction/groundwater transport models. *Mathematics and Computers in Simulation*
434 53(1-2) 113-127.
- 435 Barry, D.A., Miller, C.T., Culligan-Hensley, P.J., 1996. Temporal discretisation errors in non-
436 iterative split-operator approaches to solving chemical reaction groundwater
437 transport models. *Journal of Contaminant Hydrology* 22(1-2) 1-17.
- 438 Barry, D.A., Miller, C.T., Culligan, P.J., Bajracharya, K., 1997. Analysis of split operator
439 methods for nonlinear and multispecies groundwater chemical transport models.
440 *Mathematics and Computers in Simulation* 43(3-6) 331-341.
- 441 Barry, D.A., Starr, J.L., Parlange, J.Y., Braddock, R.D., 1983. Numerical analysis of the snow-
442 plow effect. *Soil Science Society of America Journal* 47(5) 862-868.
- 443 Bear, J., 1972. *Dynamics of Fluids in Porous Media*. Elsevier Scientific Publishing Co, New
444 York, 764 pp.
- 445 Bear, J., 2007. *Hydraulics of Groundwater*, Reprint ed. Dover Publications, Mineola, NY, 569
446 pp.
- 447 Bear, J., Bachmat, Y., 1998. *Introduction to Modeling of Transport Phenomena in Porous*
448 *Media*, Reprinted ed. Kluwer, Dordrecht, 553 pp.
- 449 Brook, G.A., Folkoff, M.E., Box, E.O., 1983. A world model of soil carbon-dioxide. *Earth*
450 *Surface Processes and Landforms* 8(1) 79-88.
- 451 Brooks, R.H., Corey, A.T., 1964. *Hydraulic properties of porous media*, Hydrological Paper.
452 Civil Engineering Department, Colorado State University: Fort Collins, Colorado.
- 453 Brussaard, L., Pulleman, M.M., Ouédraogo, É., Mando, A., Six, J., 2007. Soil fauna and soil
454 function in the fabric of the food web. *Pedobiologia* 50(6) 447-462.
- 455 Charlton, S.R., Parkhurst, D.L., 2010. Modules based on the geochemical model PHREEQC for
456 use in scripting languages and reactive-transport calculations. *Environmental*
457 *Modelling & Software*, under review.
- 458 COMSOL Multiphysics[®], 2008a. Pesticide transport and reaction in soil, Earth Science
459 Module Model Library.
- 460 COMSOL Multiphysics[®], 2008b. Variably saturated flow and transport: Sorbing solute, Earth
461 Science Module Model Library.
- 462 COMSOL Multiphysics[®], 2010. <http://www.comsol.com/>, last accessed: 22.06.2010.
- 463 Corey, A.T., Auvermann, B.W., 2003. Transport by advection and diffusion revisited. *Vadose*
464 *Zone Journal* 2(4) 655-663.
- 465 Donea, J., Huerta, A., 2004. *Finite Element Methods for Flow Problems*. Wiley, England, 350
466 pp.

467 Dzombak, D.A., Morel, F.M.M., 1990. Surface Complexation Modeling : Hydrous Ferric
468 Oxide. Wiley, New York, 393 pp.

469 Feddes, R.A., Kowalik, P.J., Zaradny, H., 1978. Simulation of Field Water Use and Crop Yield.
470 Pudoc, Wageningen.

471 Freedman, V., Ibaraki, M., 2002. Effects of chemical reactions on density-dependent fluid
472 flow: on the numerical formulation and the development of instabilities. *Advances in*
473 *Water Resources* 25(4) 439-453.

474 Gärdenäs, A.I., Hopmans, J.W., Hanson, B.R., Šimůnek, J., 2005. Two-dimensional modeling
475 of nitrate leaching for various fertigation scenarios under micro-irrigation.
476 *Agricultural Water Management* 74(3) 219-242.

477 Gustafsson, J.P., 2010. Visual MINTEQ version 3.0,
478 <http://www.lwr.kth.se/English/OurSoftware/vminteq/>, last accessed: 22.06.2010.

479 Hanson, B.R., Šimůnek, J., Hopmans, J.W., 2006. Evaluation of urea-ammonium-nitrate
480 fertigation with drip irrigation using numerical modeling. *Agricultural Water*
481 *Management* 86(1-2) 102-113.

482 Harbaugh, A.W., Banta, E.R., Hill, M.C., McDonald, M.G., 2000. MODFLOW-2000, the U.S.
483 Geological Survey modular ground-water model: User guide to modularization
484 concepts and the ground-water flow process. U.S. Geological Survey.

485 Hedrich, R., Schroeder, J.I., 1989. The physiology of ion channels and electrogenic pumps in
486 higher-plants. *Annual Review of Plant Physiology and Plant Molecular Biology* 40
487 539-569.

488 Hiemstra, T., van Riemsdijk, W.H., Bolt, G.H., 1989. Multisite proton adsorption modeling at
489 the solid-solution interface of (hydr)oxides - A new approach. 1. Model description
490 and evaluation of intrinsic reaction constants. *Journal of Colloid and Interface*
491 *Science* 133(1) 91-104.

492 Huyakorn, P.S., Pinder, G.F., 1983. *Computational Methods in Subsurface Flow*. Academic
493 Press, London, UK, 473 pp.

494 Jacques, D., Šimůnek, J., 2010. Notes on HP1 - a software package for simulating variably-
495 saturated water flow, heat transport, solute transport and biogeochemistry in
496 porous media Waste and Disposal, SCK•CEN: Mol, Belgium.

497 Jacques, D., Šimůnek, J., Mallants, D., van Genuchten, M.T., 2006. Operator-splitting errors
498 in coupled reactive transport codes for transient variably saturated flow and
499 contaminant transport in layered soil profiles. *Journal of Contaminant Hydrology*
500 88(3-4) 197-218.

501 Jacques, D., Šimůnek, J., Mallants, D., van Genuchten, M.T., 2008. Modeling coupled
502 hydrologic and chemical processes: Long-term uranium transport following
503 phosphorus fertilization. *Vadose Zone Journal* 7(2) 698-711.

504 Langmuir, D., 1997. *Aqueous Environmental Geochemistry*. Prentice Hall, Upper Saddle
505 River, 600 pp.

506 Letey, J., Kemper, W.D., Noonan, L., 1969. Effect of osmotic pressure gradients on water
507 movement in unsaturated soil. *Soil Science Society of America Proceedings* 33(1) 15-
508 18.

509 Mao, X., Prommer, H., Barry, D.A., Langevin, C.D., Panteleit, B., Li, L., 2006. Three-
510 dimensional model for multi-component reactive transport with variable density
511 groundwater flow. *Environmental Modelling & Software* 21(5) 615-628.

512 Matlab[®], 2010. The MathWorks, <http://www.mathworks.com/>, last accessed: 22.06.2010.

513 Mayer, K.U., Frind, E.O., Blowes, D.W., 2002. Multicomponent reactive transport modeling
514 in variably saturated porous media using a generalized formulation for kinetically
515 controlled reactions. *Water Resources Research* 38(9) 131-1321.

516 Meeussen, J.C.L., 2003. ORCHESTRA: An object-oriented framework for implementing
517 chemical equilibrium models. *Environmental Science & Technology* 37(6) 1175-1182.

518 Miller, C.T., Christakos, G., Imhoff, P.T., McBride, J.F., Pedit, J.A., Trangenstein, J.A., 1998.
519 Multiphase flow and transport modeling in heterogeneous porous media: Challenges
520 and approaches. *Advances in Water Resources* 21(2) 77-120.

521 Millington, R.J., Quirk, J.P., 1961. Permeability of porous solids. *Transactions of the Faraday*
522 *Society* 57 1200-1207.

523 Parkhurst, D.L., 2010. Personal Communication.

524 Parkhurst, D.L., Appelo, C.A.J., 1999. User's guide to PHREEQC (version 2): A computer
525 program for speciation, batch-reaction, one-dimensional transport, and inverse
526 geochemical calculations. U.S. Geological Survey: Denver, Colorado.

527 Parkhurst, D.L., Kipp, K.L., Engesgaard, P., Charlton, S.R., 2004. PHAST - A Program for
528 simulating ground-water flow, solute transport, and multicomponent geochemical
529 reactions. U.S. Geological Survey: Denver, Colorado.

530 Perrochet, P., Berod, D., 1993. Stability of the standard Crank-Nicolson-Galerkin scheme
531 applied to the diffusion-convection equation - Some new insights. *Water Resources*
532 *Research* 29(9) 3291-3297.

533 Prommer, H., Barry, D.A., Zheng, C., 2003. MODFLOW/MT3DMS-based reactive
534 multicomponent transport modeling. *Ground Water* 41(2) 247-257.

535 Prommer, H., Davis, G.B., Barry, D.A., 1999. PHT3D - A three-dimensional biogeochemical
536 transport model for modelling natural and enhanced remediation, In: Johnston, C.D.
537 (Ed.), *Contaminated Site Remediation: Challenges Posed by Urban and Industrial*
538 *Contaminants*. Centre for Groundwater Studies: Fremantle, Western Australia, pp.
539 351-358.

540 Saaltink, M.W., Batlle, F., Ayora, C., Carrera, J., Olivella, S., 2004. RETRASO, a code for
541 modeling reactive transport in saturated and unsaturated porous media. *Geologica*
542 *Acta* 2(3) 235-251.

543 Šimůnek, J., Bradford, S.A., 2008. Vadose zone modeling: Introduction and importance.
544 *Vadose Zone Journal* 7(2) 581-586.

545 Šimůnek, J., Hopmans, J.W., 2009. Modeling compensated root water and nutrient uptake.
546 *Ecological Modelling* 220(4) 505-521.

547 Šimůnek, J., Jacques, D., van Genuchten, M.T., Mallants, D., 2006. Multicomponent
548 geochemical transport modeling using HYDRUS-1D and HP1. *Journal of the American*
549 *Water Resources Association* 42(6) 1537-1547.

550 Šimůnek, J., Šejna, M., Saito, H., Sakai, M., van Genuchten, M.T., 2009. The HYDRUS-1D
551 software package for simulating the movement of water, heat, and multiple solutes
552 in variably saturated media, Version 4.0. Department of Environmental Sciences,
553 University of California Riverside: Riverside, California.

554 Šimůnek, J., Šejna, M., van Genuchten, M.T., 1999. The HYDRUS-2D software package for
555 simulating the two-dimensional movement of water, heat, and multiple solutes in
556 variably-saturated media, Version 2.0. Department of Environmental Sciences,
557 University of California Riverside: Riverside, California.

558 Šimůnek, J., Vogel, T., van Genuchten, M.T., 1994. The SWMS-2D code for simulating water
559 flow and solute transport in two-dimensional variably saturated media, Version 1.21.
560 U.S. Salinity Laboratory: Riverside, CA.

561 Steefel, C.I., MacQuarrie, K.T.B., 1996. Approaches to modeling of reactive transport in
562 porous media, In: Lichtner, P.C., Steefel, C.I., Oelkers, E.H. (Eds.), *Reactive Transport
563 in Porous Media. Reviews in Mineralogy*, 34. Mineralogical Society of America:
564 Washington DC, pp. 82-129.

565 Valocchi, A.J., Malmstead, M., 1992. Accuracy of operator splitting for advection-dispersion-
566 reaction problems. *Water Resources Research* 28(5) 1471-1476.

567 van der Lee, J., 1998. Thermodynamic and mathematical concepts of CHESS. Ecole des
568 Mines de Paris: Fontainebleau, France.

569 van Genuchten, M.T., 1980. Closed-form equation for predicting the hydraulic conductivity
570 of unsaturated soils. *Soil Science Society of America Journal* 44(5) 892-898.

571 Voss, C.I., Provost, A.M., 2008. SUTRA: A model for saturated-unsaturated, variable-density
572 ground-water flow with solute or energy transport. U.S. Geological Survey: Reston,
573 Virginia.

574 Vrugt, J.A., Hopmans, J.W., Šimůnek, J., 2001. Calibration of a two-dimensional root water
575 uptake model. *Soil Science Society of America Journal* 65(4) 1027-1037.

576 Wissmeier, L., Barry, D.A., 2010. Implementation of variably saturated flow into PHREEQC
577 for the simulation of biogeochemical reactions in the vadose zone. *Environmental
578 Modelling & Software* 25(4) 526-538.

579 Wissmeier, L., Brovelli, A., Robinson, C., Stagnitti, F., Barry, D.A., 2009. Pollutant fate and
580 transport in the subsurface, *Modelling of Pollutants in Complex Environmental
581 Systems*. ILM Publications, pp. 99-143.

582 Yeh, G.T., Tripathi, V.S., 1989. A critical evaluation of recent developments in
583 hydrogeochemical transport models of reactive multi-chemical components. *Water
584 Resources Research* 25(1) 93-108.

585 Yukselen, Y., Kaya, A., 2006. Prediction of cation exchange capacity from soil index
586 properties. *Clay Minerals* 41(4) 827-837.

587

588

Table

Table 1

Geochemical solution properties. Master species concentrations in mol(kg water)⁻¹, truncated to 2 digits.

	Fertilizer solution	Irrigation water	Initial soil solution
pH	3.844	5.659	4.660
pe	16.78	14.96	15.96
O	56.12	55.51	55.51
H	111.34	111.01	111.02
P	0.15	0.00	0.00
K	0.15	0.00	0.00
Amm	3.62×10^{-2}	0.00	0.00
Urea	7.25×10^{-2}	0.00	0.00
N	3.62×10^{-2}	0.00	0.00
C	1.04×10^{-5}	1.30×10^{-5}	1.10×10^{-3}

Figure Captions

Fig. 1. Program flow and structure.

Fig. 2. Simulation domain with finite element mesh for pesticide simulation. The source zone is indicated by the thick line at $y = 0$.

Fig. 3. Aldicarb reaction chain.

Fig. 4. Comparison of concentrations from the coupling procedure and COMSOL alone eight d after beginning of infiltration.

Fig. 5. Simulation domain with finite element mesh for drip irrigation simulation.

Fig. 6. Normalized root distribution according to the Vrugt model (Vrugt et al., 2001) with parameters from Hanson et al. (2006).

Fig. 7. Moisture contents at 0 and 1.15 d, i.e., the beginning and end of the first irrigation period; white contours: lines of equal water contents.

Fig. 8. Solution master species concentrations 3.88, 4.63, 5, 7 and 28 d after beginning of fertigation cycles.

Fig. 9. Moisture contents, pH and exchanger composition 3.88, 4.63, 5, 7 and 28 d after beginning of fertigation cycles.

